GNSS Constellation Performance Using ARAIM with Inclined Geosynchronous Satellite and Low-Earth-Orbit Satellite Augmentation

Sam Pullen, Sherman Lo, Isaiah Colobong, Sukrut Oak, Juan Blanch, Todd Walter
Stanford University
Mark Crews, Robert Jackson, Stephen Young, Kevin Huttenhoff
Lockheed Martin

Abstract

In previous work (Pullen 2022), we introduced the concept of augmenting GPS with six inclined geosynchronous satellites (I-GEOs) that would provide GPS-Block-III-quality military and civil ranging signals along with conveying Satellite-based Augmentation System (SBAS) messages to users. This would create a new means to distribute SBAS messages globally and would support Advanced Receiver Autonomous Integrity Monitoring (ARAIM) for users not equipped to use SBAS. This paper examines multiple configurations of I-GEO satellites augmenting GPS satellites and includes augmentation by satellites in Low Earth Orbit (LEO). For each arrangement of satellites, the Stanford MAAST GNSS simulation software package is used to evaluate the protection levels and the availability of integrity for aviation LPV approaches (to a minimum decision height of 250 ft) for ARAIM users. MAAST computes PLs and availability for a global grid of military (dual-frequency M-code and/or PRS) and civil (dual-frequency L1/L5 or equivalent) user locations separated by 5 degrees of latitude and longitude. Contour plots of LPV availability, Vertical Protection Level (VPL), and Horizontal Protection Level (VPL and HPL) are generated for each combination of I-GEO and other GNSS satellites. In addition, sorted (by magnitude) values of VPL and HPL are plotted for example locations in the user grid to illustrate the sensitivity of VPL and HPL to the poorest satellite geometries before and after I-GEOs or LEOs are included.

1. INTRODUCTION

Integrity for safety-of-life applications of GNSS such as civil aviation is provided today by Satellite-based Augmentation Systems (SBAS) and various forms of Receiver Autonomous Integrity Monitoring (RAIM). Today's SBAS provides only single-frequency (L1 C./A code) corrections, although dual-frequency SBAS that also provides corrections on L5/E5a may become available in the next decade. Users not supported by existing SBAS, such as military users of L1/L2 P/Y and M codes, can take advantage of Advanced Receiver Autonomous Integrity Monitoring (ARAIM), which extends the capabilities of earlier forms of RAIM to multiple-failure scenarios.

The version of ARAIM being developed for civil aviation users ((Blanch, 2015), (Milestone 3, 2016) depends on using signals from multiple GNSS constellations (typically at least GPS and Galileo) to provide high availability for demanding horizontal (e.g., RNP 0.1) and vertical (e.g., LPV) phases of flight. However, it is likely that at least U.S. military users will be restricted from using GNSS signals not provided or authorized by the U.S. government. This limitation has been explored in our previous work on ARAIM, where the use of Galileo in a limited "constellation check" form was evaluated (Katz, 2021). We have also evaluated improvements to ARAIM performance based upon establishing lower error bounds in the Integrity Support Message (ISM) provided by ARAIM based upon more intensive GNSS ground monitoring and faster ISM message updates (Pullen, 2021).

In Pullen (2022), we took a different approach by considering the benefits to both civil and military user integrity of augmenting GNSS with a constellation of Inclined Geosynchronous (I-GEO) satellites: two satellites in each of three planes 120 degrees apart inclined by 55 degrees (the same inclination angle as GPS). These satellites would provide GPS-quality L1, L2, and L5 ranging measurements while also proving L1, L2 and L5 SBAS corrections. Figure 1, updated from the result in Pullen (2022), shows that the provision of dual-frequency SBAS corrections from 25 globally-distributed reference stations through these six I-GEO satellites provides near-100% availability
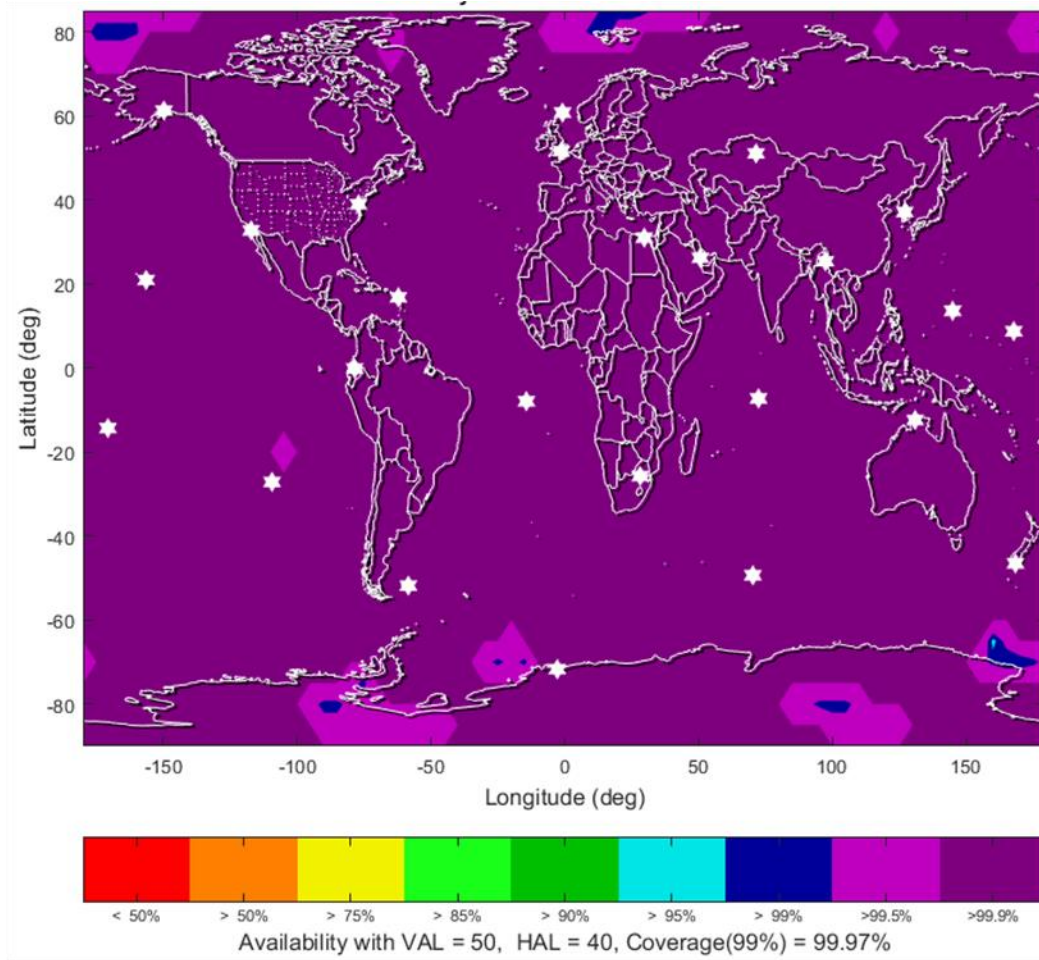
Figure 1: *LPV User Availability Based upon Dual-Frequency SBAS Corrections, 6 I-GEO Satellites, and 25 SBAS Reference Stations (shown as white stars) (updated from (Pullen, 2022))*

of LPV approach operations under limited visibility down to 250 ft above the runway threshold. LPV availability in these simulations is determined by having both the Vertical Protection Level (VPL) below a Vertical Alert Limit of 50 meters and the 2-D Horizontal Protection Level (HPL) below a Horizontal Alert Limit of 40 meters. In Figure 1, users are simulated at a grid of locations separated by 5 degrees in latitude and longitude. This figure shows that practically all user locations around the world have better than 99% availability of LPV operations, meaning that VPL is below VAL and HPL is below VAL at more than 99% of time epochs over one day of repeatable GPS and I-GEO satellite geometries. This is demonstrated by both the colors of the availability contours and the "Coverage(99%) statistic at the lower right of Figure 1, which gives the percentage of user locations with availability at or above 99% as 99.97%.

In Figure 1, most of the world is shown in dark purple, representing an availability exceeding 99.9%. Since only 288 time epochs were simulated over one day (with 5 minutes between epochs), those locations had availability for every epoch simulated. Also note that excellent availability is provided all the way to the poles, which is not possible in conventional SBAS because corrections broadcast by geostationary satellites near the equator cannot be reliable received in the far polar regions. Because LPV availability with I-GEO-provided SBAS corrections is so good, this paper focuses on ARAIM performance for users unable to apply dual-frequency SBAS and thus reliant on the additional geometry redundancy provided by I-GEO or LEO augmentations to GNSS.

2. MAAST SIMULATION PROCEDURE FOR ARAIM

Parameter	GPS Commitment	GPS, I-GEO, LEO SVs (with additional ground monitoring)
URA	in Nav Data (ICD table)	URA = 1.0 m; URE = 0.63 m; bias = 0.35 m
URA Threshold	4.42 × URA	URA Threshold based on P_{sat}
R_{sat}	10^{-5} / hour	R_{sat} = 5 × 10^{-7} / hour
P_{sat}	10^{-5}	P_{sat} = 5 × 10^{-7}
P_{const}	10^{-8}	P_{const} = 2.5 × 10^{-9}
MFD	1 hour	MFD = 1 hour
TTA	10 seconds	TTA = 10 seconds

Figure 2: *SIS Error and Fault-Model Parameters Used in MAAST ARAIM Simulations (Pullen, 2022)*

The ARAIM version of Matlab Algorithm Availability Simulation Tool (MAAST) developed by Stanford is used to determine VPL, HPL, and the resulting LPV availability of each user location in the same manner as in Pullen (2021) and Pullen (2022). Briefly, MAAST simulates the satellite geometries observed by a grid of user locations around the world based on Yuma-almanac-formatted definitions of GNSS, GEO, and LEO satellite constellations. At a given time epoch, a user error model is computed for each satellite visible at each user location, which allows the ARAIM algorithm ((Blanch, 2015), (Milestone 3, 2016)) to generate a variety of performance indicators for each user location at that time. These indicators (including VPL and HPL) are stored for each user location and time epoch so that post-processing after the satellite geometry simulation completes can determine the availability of integrity for each location, which is the number of epochs in which both VPL ≤ VAL and HPL ≤ HAL for the operation in question (LPV) divided by the total number of epochs.

Figure 2 from Pullen (2022) shows the signal-in-space (SIS) components of the error and prior-probability-of-(integrity)-failure models used for GPS (MEO) satellites and I-GEO and LEO satellite augmentations in these simulations. The numbers for GPS satellites in the yellow-highlighted column to the left are those promised by the U.S. operators of GPS to the International Civil Aviation Organization in support of ARAIM (ICAO, 2020). The improved numbers highlighted in green on the right are those used in these simulations and represent additional ground monitoring of the GPS and augmentation satellites with ISM updates at least daily if needed (Katz, 2021). These values provide the potential high availability of vertical ARAIM (meaning ARAIM in support of applications with demanding requirements on vertical position, as for LPV) even without GEO or LEO augmentations, as will be shown in Section 4.1. The benefit of adding I-GEO or LEO ranging satellites with, for simplicity, the same error and fault-probability characteristics as GPS satellites, is to have this availability approach the ideal results achievable with SBAS corrections as shown in Figure 1.

3. INCLINED GEOSYNCHRONOUS SATELLITE (I-GEO) COMBINATIONS

Figure 3 (from (Pullen, 2022)) shows the initial configuration of 6 I-GEOs in three planes along with the 25 SBAS reference stations used to generate the availability result in Figure 1. As noted before, each of the three I-GEO planes is separated by 120 degrees of right ascension ($\Delta\Omega$), while the change in mean anomaly (ΔM) is 180 degrees between satellites in the same plane and 90 degrees between adjacent planes. This pattern is workable, but it introduces asymmetry in the results because the adjacent orbit planes at 120 degrees East and West longitude (far right and far left in Figure 3, respectively) have the same in-plane satellite locations at the same time.
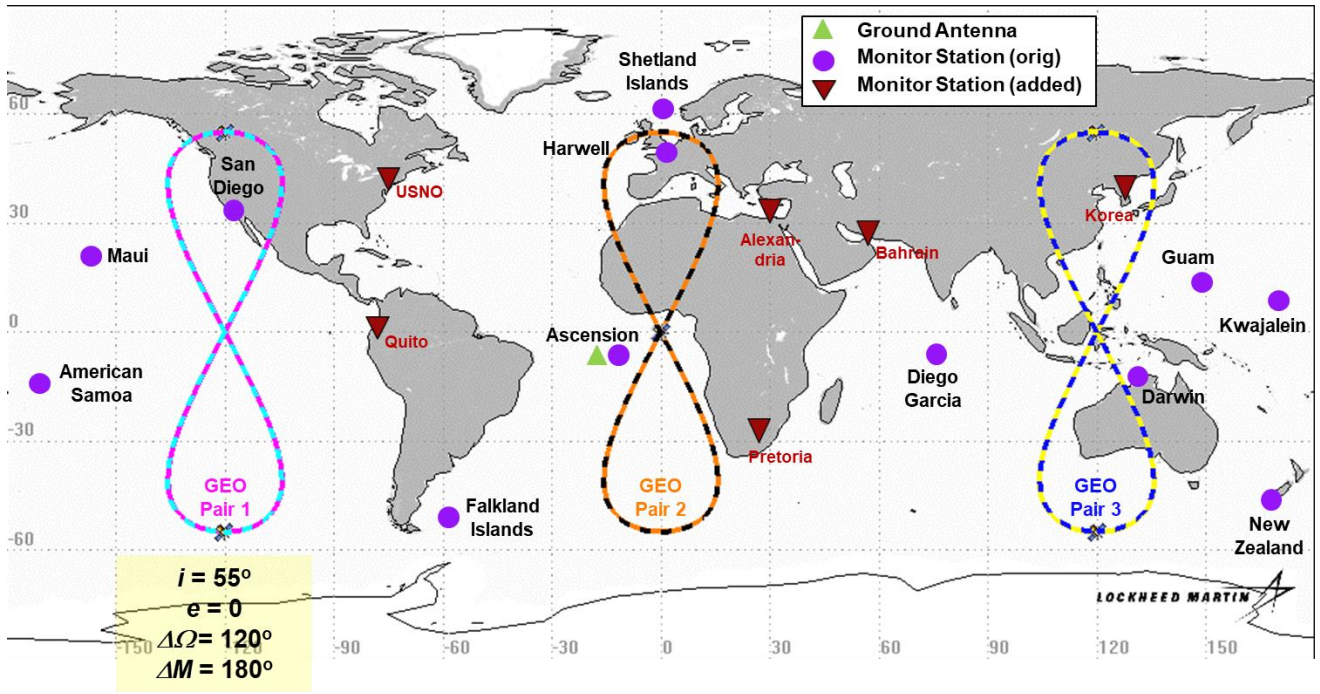
Figure 3: *Original I-GEO Satellite Configuration and 25 SBAS Reference Station Locations (Pullen, 2022)*

Therefore, for this study, the baseline I-GEO configuration (here called "baseline" and denoted as "3 × 2", corresponding to 3 planes with two satellites each) was modified to be the same except that ΔM between adjacent planes was reduced to 60 degrees (it remains 180 degrees within each plane). Table 1 shows the right ascension of the ascending node (RAAN, or Ω) and mean anomaly (M) parameters of each of the six satellites in this configuration. This combination produces protection level and availability results that are globally symmetric (to first order), as expected.

Table 1: *Satellite Orbit Parameters for Baseline I-GEO Combination ("3 × 2")*

I-GEO ID #	RAAN (deg)	Mean Anomaly (deg)
81	0	0
82	0	180
83	120	60
84	120	240
85	240	120
86	240	300

Alternative I-GEO Combinations 1 and 2 are both based on this baseline configuration. Alterative Combination 1, shown in Table 2, adds one satellite to each of the three planes in the baseline configuration, resulting in nine total satellites ("3 × 3") and modified mean anomalies. The in-plane mean anomaly change (ΔM_{inside}) is reduced from 180 to 120 degrees to equally distribute three satellites within each plane, while the between-plane mean anomaly change ($\Delta M_{between}$) is reduced from 60 to 40 degrees to maintain a uniform offset across the world. Alternative I-GEO Combination 2, shown in Table 3, instead retains two satellites in each plane (and $\Delta M_{inside} = 180$ degrees) but adds a fourth plane of two satellites (creating a total of eight satellites in a "4 × 2" arrangement) with a change in right ascension between planes of 90 degrees and a between-plane mean anomaly change ($\Delta M_{between}$) of 45 degrees to fit them in uniformly.

Table 2: *Satellite Orbit Parameters for Alternative I-GEO Combination 1 ("3 × 3")*

I-GEO ID #	RAAN (deg)	Mean Anomaly (deg)
81	0	0
82	0	120
83	0	240
84	120	40
85	120	160
86	120	280
87	240	80
88	240	200
89	240	320

Table 3: *Satellite Orbit Parameters for Alternative I-GEO Combination 2 ("4 × 2")*

I-GEO ID #	RAAN (deg)	Mean Anomaly (deg)
81	0	0
82	0	180
83	90	45
84	90	225
85	180	90
86	180	270
87	270	135
88	270	315

In addition, a third alternative was created and simulated by combining the changes made in Alternative Combinations 1 and 2, meaning that the I-GEO constellation was expanded from three to four planes, and the number of satellites in each plane was also increased from 2 to three (thus "4 × 3"). This combination has 12 I-GEO satellites in total. Because of the additional expense of launching and maintaining 12 I-GEO satellites instead of eight or nine, the fact that LPV availability is not significantly improved by this alternative, and space limitations in this paper, results for it are omitted.

4. RESULTS FOR GPS AUGMENTED WITH I-GEO COMBINATIONS

4.1 GPS Satellites Only

ARAIM results for LPV availability for GPS without I-GEO or LEO satellite augmentation were provided in Pullen (2022) for the baseline 24-Slot GPS constellation defined in Table 3.2-1 of the *GPS SPS Performance Standard* (SPS, 2020). These results are extended to two versions of the expandable 24-Slot constellation, which contains 27 and 30 satellites, respectively. These two expansions of the 24-Slot constellation are shown in Table 3.2-2 of SPS (2020). The 27-Slot constellation (denoted as "24+3" in this paper) is created by implementing the first three rows of this table; i.e., replacing the GPS satellites in orbit slots B1, D2, and F2 with two nearby satellites in slots B1F, B1A, D2F, D2A, F2F, and F2A. The 30-Slot constellation is created from the 27-Slot version by additionally replacing the GPS satellites in orbit slots A2, C4, and E3 with two nearby satellites in slots A2F, A2A, C4F, C4A, E3F, and E3A. In each of the modified orbit planes, the "nearby" satellites are within 10 to 20 degrees on either side of the removed
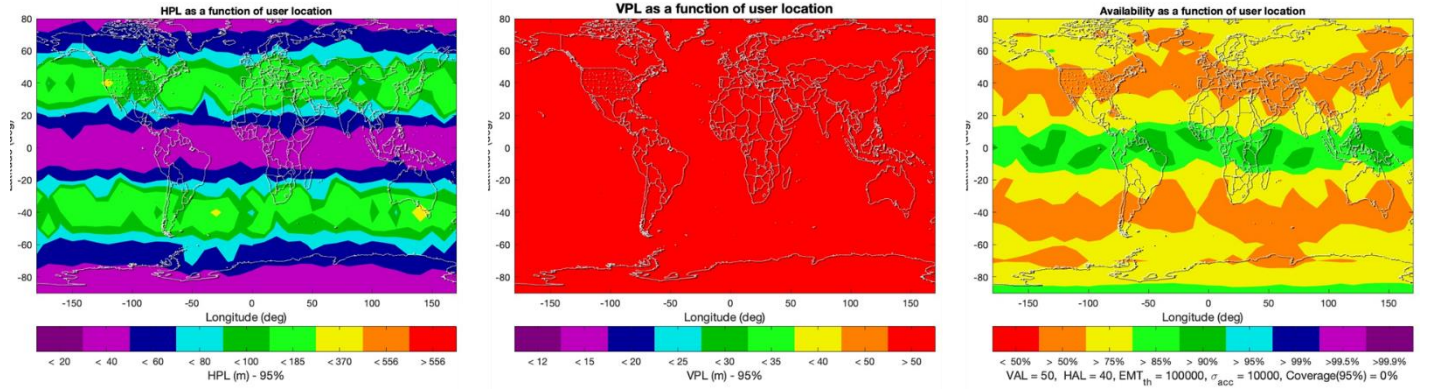
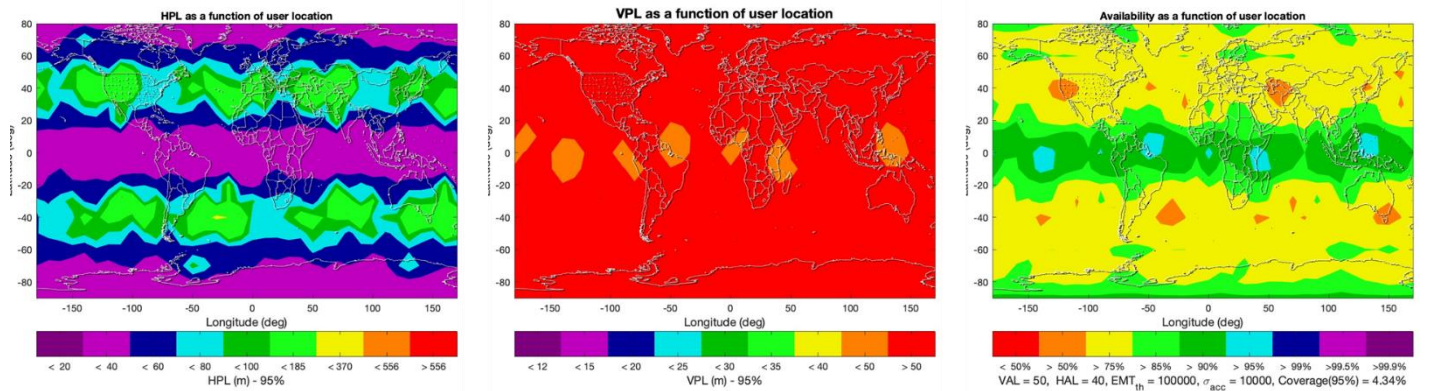**Figure 4:** *HPL, VPL, and LPV Availability Contours for Unaugmented 24-Slot GPS Constellation*

Figure 5: *HPL, VPL, and LPV Availability Contours for Unaugmented 27-Slot (24+3) GPS Constellation*
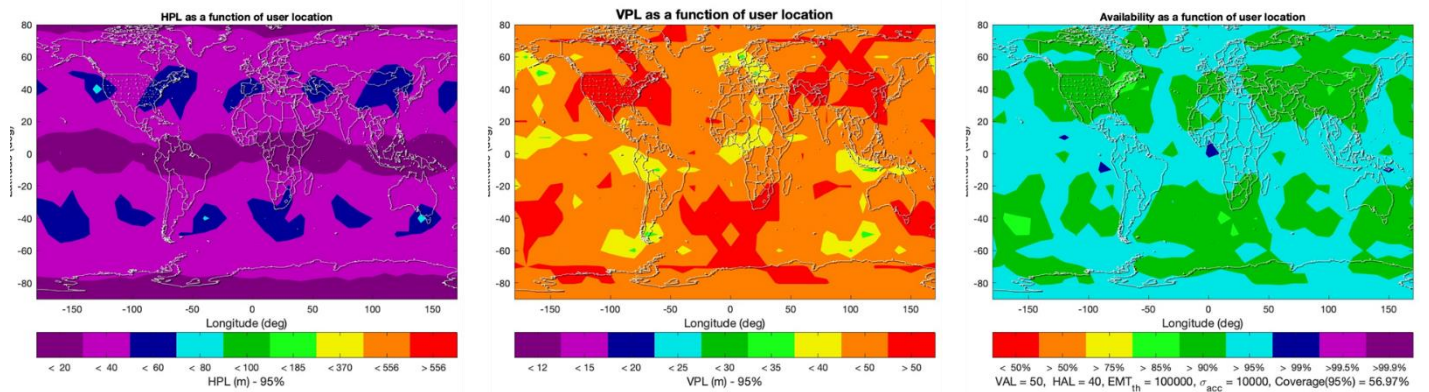

Figure 6: *HPL, VPL, and LPV Availability Contours for Unaugmented 30-Slot (24+6) GPS Constellation*

satellite. This provides a small amount of additional geometric redundancy but does not always improve on the original 4-satellite-per-plane configuration of the 24-Slot constellation.

Figure 4 shows, from left to right, contour plots of HPL, VPL, and LPV availability for the use of vertical ARAIM with the 24-Slot GPS constellation, the SIS parameters shown in Figure 3, and no I-GEO or LEO augmentation satellites. Note that these contours (and all contours that follow) are at the 95th percentile ("95%"), meaning that the colors shown on each map indicate PL values or
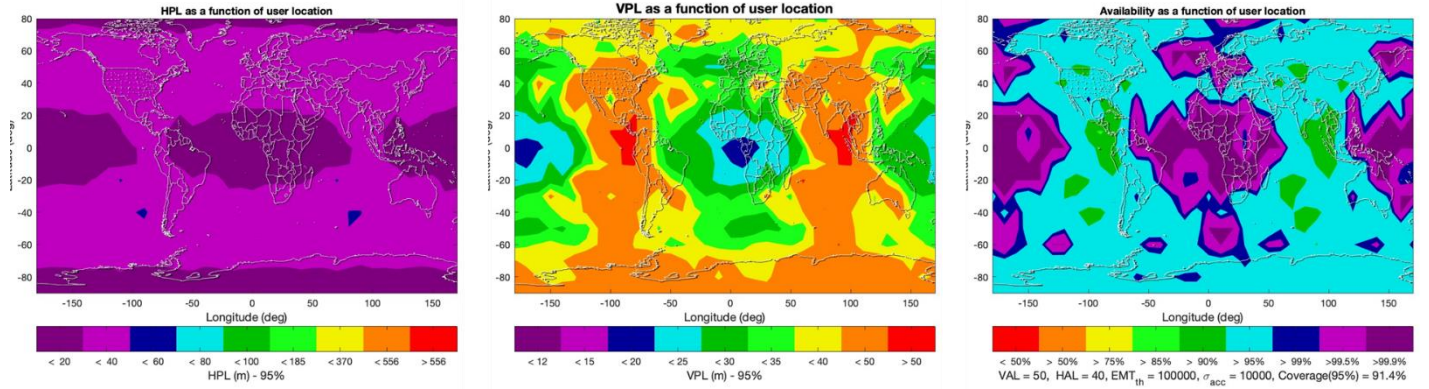
Figure 7: *HPL, VPL, and LPV Availability Contours for 24-Slot GPS Constellation and Baseline I-GEO Combination ("3 × 2")*
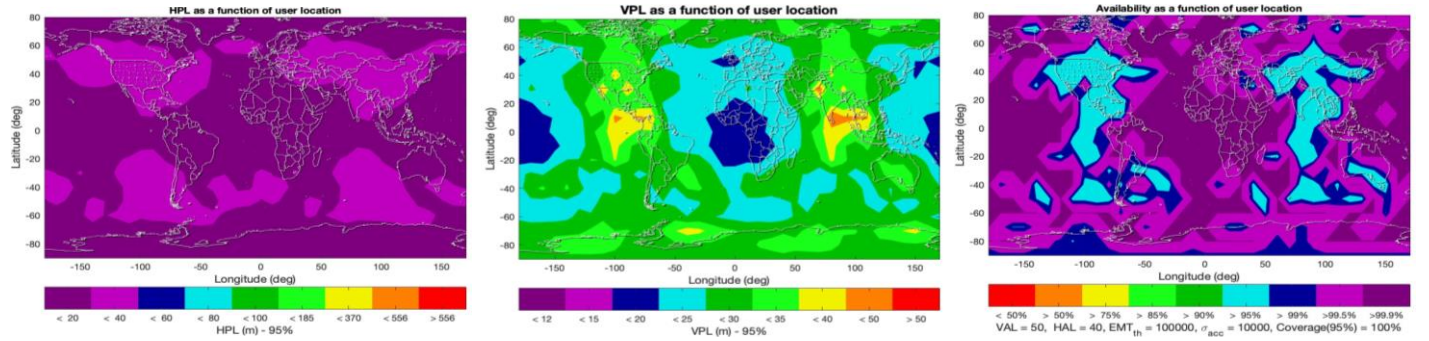

Figure 8: *HPL, VPL, and LPV Availability Contours for 30-Slot (24+6) GPS Constellation and Baseline I-GEO Combination ("3 × 2")*

availability percentages that are exceeded only 5% of the time at the location underneath. The middle plot is most striking, as it is solid red and indicates that, not surprisingly, ARAIM cannot support 95% VPLs below 50 meters anywhere on Earth. As a result, LPV availability in this scenario cannot exceed 95% anywhere on Earth. This is confirmed by the right-hand plot, which shows levels of availability between 50% and just over 90% depending on location. The locations with the highest availability are those with the lowest 95% HPL contours, as shown in the left-hand plot, and these are mostly in equatorial and polar regions.

Figure 5 shows the same contour plots for the 27-Slot (24+3) constellation without I-GEO or LEO augmentation. It shows noticeable but relatively minor improvements over the 24-Slot results. Figure 6 shows these contour plots for the 30-Slot (24+6) constellation without augmentation. It shows much more significant improvement, as most of the world now achieves 95% VPLs lower than 50 or even 40 meters. This, combined with similar improvements in HPL, translates into LPV availability exceeding 95% for about 57% of the world, with most of the remaining locations exceeding 90% availability.

The results in Figure 6 are quite good for GPS unaugmented by other GNSS constellations, GEOs, or LEOs. However, they fall well short of the 99.9% level availability desired for at least part of the world, and they depend on the additional offline ground monitoring that supports the ISM values shown in Figure 2. Therefore, geometry augmentation by satellites that can be used by military and other non-SBAS users would be very helpful, aside from the benefits of I-GEOs in providing SBAS corrections.

4.2 GPS with Baseline I-GEO Combination ("3 × 2")

Figure 7 shows the 95% HPL/VPL/LPV availability contour plots for the 24-Slot GPS constellation augmented by the baseline I-GEO combination defined in Table 1. The addition of I-GEOs greatly improves the VPL contours compared to all three versions of the GPS-only constellation. Longitudinal bands of improved (blue-green contours, with 95% VPLs from 15 to 35 meters) and less-(yellow-orange contours, with 95% VPLs from 35 to 50 meters) stand out and show the influence of the I-GEO satellite locations relative to users. A similar pattern is visible in the HPL and LPV availability contours, where "favored" locations exceeding 99.5%

LPV availability compared to "less favored" ones only exceeding 95% availability. Of course, both types of locations improve greatly compared to the same GPS constellation without I-GEOs (Figure 4), illustrating their benefits for ARAIM very clearly. LPV availability in Figure 7 is also much better than even the 30-Slot unaugmented GPS constellation in Figure 6.

Figure 8 shows the 95% HPL/VPL/LPV availability contour plots for the 30-Slot (24+6) GPS constellation augmented by I-GEO Combination 1 (results for the 27-Slot constellation with I-GEOs also exist but are omitted here to save space). Here, the addition of six GPS satellites reduces the distinction between "favored" and "less favored" locations created by the three-plane configuration of the six I-GEO satellites. For example, the regions with 95% VPL below 30 meters and LPV availability above 99.5% are much larger here than in Figure 7. This can also be seen in the "Coverage(95% availability)" indicator, which increases from 91.4% in Figure 7 to 99.58% in Figure 8. In other words, almost all locations on Earth have LPV availability exceeding 95% the 30-Slot + I-GEO (Combination) 1 scenario compared to just over 9 out of 10 in the 24-Slot + I-GEO 1 scenario.

Figures 9 and 10 take a different look at the behavior of VPL in the scenarios represented by Figures 7 and 8. In these figures, VPL (left) and HPL (right) are shown for each of the five selected locations shown in Table 4 over all 288 time epochs simulated over one repeatable day. In these "sorted" plots, VPL and HPL are separately sorted from highest to lowest, meaning that the order of epochs for VPL and HPL may be different. Sorting in this manner allows us to observe the percentage of epochs that fall above or below
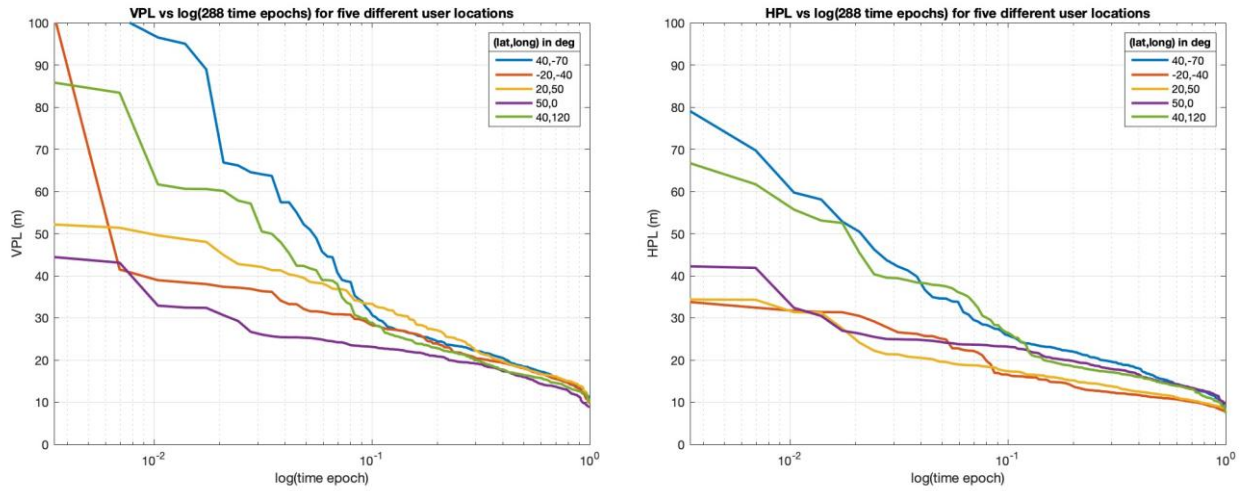

Figure 9: *Sorted VPL and HPL for 24-Slot GPS Constellation and Baseline I-GEO Combination ("3 × 2")*
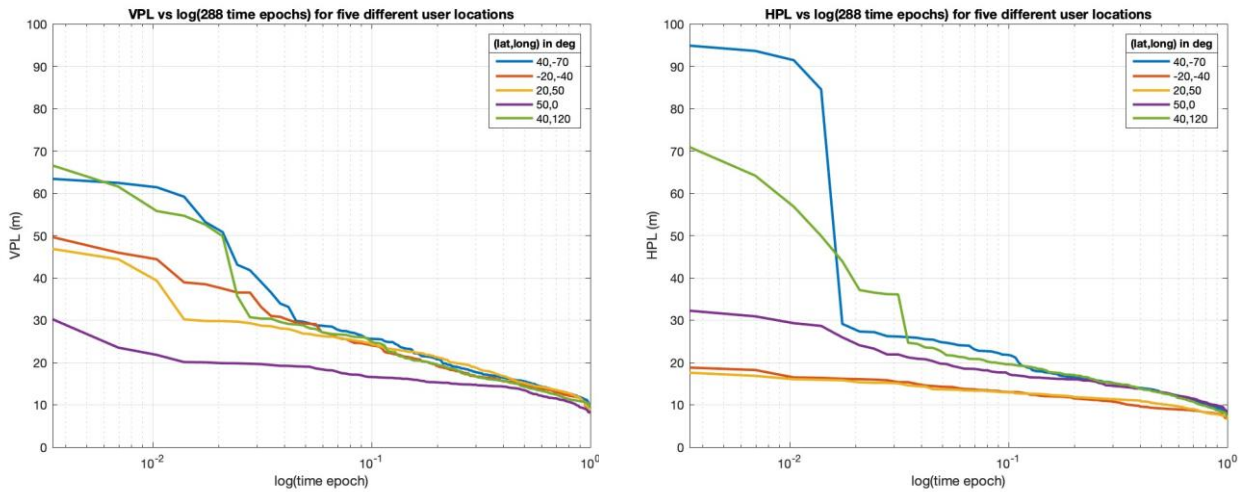

Figure 10: *Sorted VPL and HPL for 30-Slot (24+6) GPS Constellation and Baseline I-GEO Combination ("3 × 2")*

Table 4: *Five Selected User Locations and MAAST User Grid Equivalents*

Approximate User Location (latitude, longitude in degrees)	MAAST Location (latitude, longitude in degrees)
Boston (42 N, 71 W)	(40 N, 70 W)
Rio de Janeiro (23 S, 43 W)	(20 S, 40 W)
Dubai (25 N, 55 E)	(20 N, 50 E)
London (51 N, 0 E)	(50 N, 0 E)
Beijing (40 N, 117 E)	(40 N, 120 E)

any selected PL value on the y-axis, while the x-axis is plotted in semi-logarithmic form in terms of probability of exceeding the selected y-axis value. For example, in Figure 9 (for 24 GPS satellites), a VPL of 40 meters is exceeded at the green location (40° N, 120° E, near Beijing, China) with a probability of about 0.08, while the same probability for the purple location at 50° N, 0° E (near London, UK) is about 0.008. In Figure 10 (for 30 GPS satellites), these numbers improve: a VPL of 40 meters is exceeded at (40° N, 120° E) with a probability of about 0.025, while the same probability at (50° N, 0° E) is below 0.003, as all 288 epochs had VPL below 35 meters at this location for this scenario.

In general, Figures 9 and 10 show what we expect – with the addition of I-GEOs, VPL and HPL trends from lowest to highest are relatively smooth and do not show as many large "spikes" as seen without satellite augmentation (when GPS-only satellite geometries become unable to generate useful protection-level bounds). Also, while most of the user locations shown improve either slightly or significantly between Figures 9 and 10, exceptions exist, such as for the blue location (40° North, 70° West) near Boston, MA, USA, where HPL gets larger from 24 to 30 GPS satellites for the worst satellite geometries, while VPL gets smaller.

The differences between 24 and 30 GPS satellites for the same location and I-GEO combination can be more clearly seen by plotting unsorted VPL and HPL for all three GPS satellite constellation variations. "Unsorted" simply means that the PLs are plotted as they occur over time due to satellite geometry changes over the simulated day. Figures 11 and 12 show unsorted plots of VPL (left) and HPL (right) for two of the five locations shown in Figures 9 and 10: (20° N, 50° E, near Dubai) in Figure 11 and (40° North, 120° E, near Beijing) in Figure 12. Figure 11 shows that (a) PLs at this location with I-GEO augmentation are well-bounded below 35 meters, and (b) going from 24 to 30 GPS satellites generally improves PL and reduces most of the remaining small "spikes." At a few epochs, the 30-Slot result (in yellow) exceeds the 24-Slot result (in blue), but this is rare, particularly for PLs exceeding 25 meters that begin to approach LPV and LPV-200 availability limits. The improvement from 24 to 30 GPS satellites is more visible in Figure 12, as a large "spike" in VPL above 70 meters with 24 GPS satellites is not present for 30 GPS satellites. Except for the greater prevalence of small PL "spikes" in Figure 12, both locations have similar PLs below 25 meters at most times of the day.

4.3 GPS with Alternative I-GEO Combination 1 ("3 × 3")

The contour plots in Figures 13 and 14 are analogous to those in Figures 7 and 8 but for the nine-satellite, three-plane Alternative GEO Combination 1 as opposed to the baseline combination. This alternative adds one satellite each to the same three orbit planes as the baseline combination, and the benefits of these added satellites are apparent in both figures. In particular, the distinction between "favored" and "less favored" regions in Figures 7 and 8 is much weaker and is almost completely absent. This is mostly due to the performance in the "favored" regions of Figures 7 and 8 improving somewhat further and spreading out into the regions that were formally "less favored." As a result, all user locations achieve better than 95% LPV availability in both figures (i.e., for both 24-Slot and 30-Slot GPS constellations). The 30-Slot result in Figure 14 also removes most of the latitudinal bands of lower performance that are evident in Figure 13. In Figure 14, well over 90% of the world achieves a 95% HPL below 20 meters (purple), a 95% VPL below 25 meters (light or dark blue), and LPV availability at all 288 time epochs (purple).
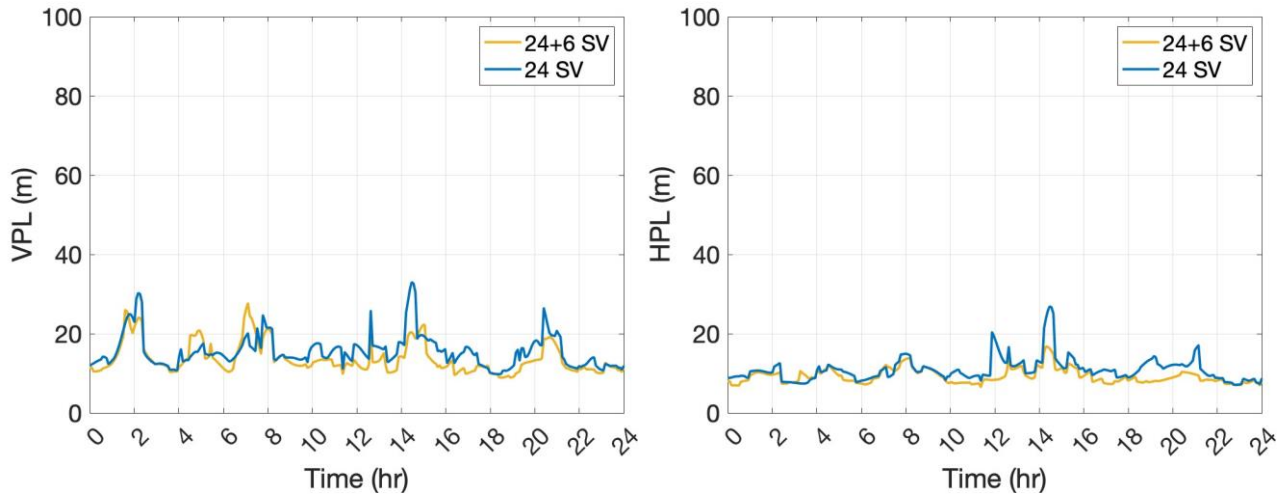
Figure 11: *Unsorted VPL and HPL at (20º N, 50º E) for and Baseline I-GEO Combination ("3 × 2") and Two GPS Variations*
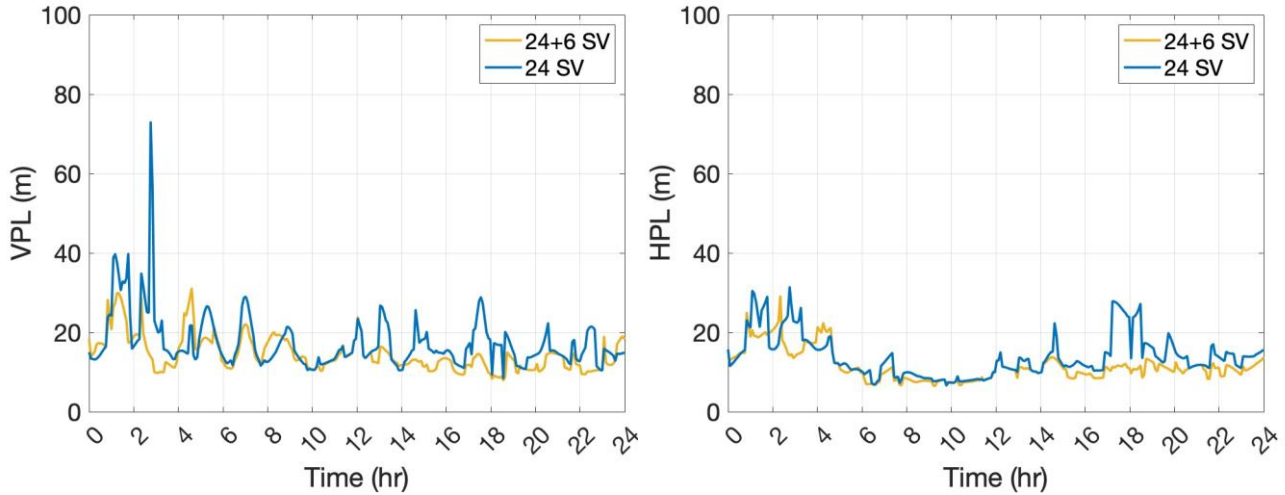

Figure 12: *Unsorted VPL and HPL at (40º N, 120º E) for Baseline I-GEO Combination ("3 × 2") and Two GPS Variations*

Sorted and unsorted PL plots have also been generated for this I-GEO combination and are summarized by Figure 15, which shows the sorted VPL and HPL for the five selected locations shown in Table 4 and 30 GPS satellites. As expected from the contour plots in Figures 13 and 14, Figure 15 shows significantly lowered PLs in general when compared to the analogous Figure 10 for the baseline I-GEO combination with 30 GPS satellites. However, closer inspection shows that one location actually does somewhat worse: the purple location at (50º N, 0º E) near London, UK. This is because the London location is on the prime meridian and sits directly under one of the three I-GEO orbit planes. Thus, adding a third satellite to the three planes does not typically increase the number of I-GEO satellites in view, and the greater distance between I-GEOs in the 3 × 2 baseline combination appears to give a small advantage over the 3 × 3 combination. Overall, Figure 15 shows that VPL for these five locations is always below 50 meters and HPL is always below 60 meters (not considering satellite outages). Along with the contour plots in Figures 13 and 14, it suggests that Alternative Combination 1 provides enough performance improvement over the baseline I-GEO combination to potentially justify its three additional I-GEO satellites.
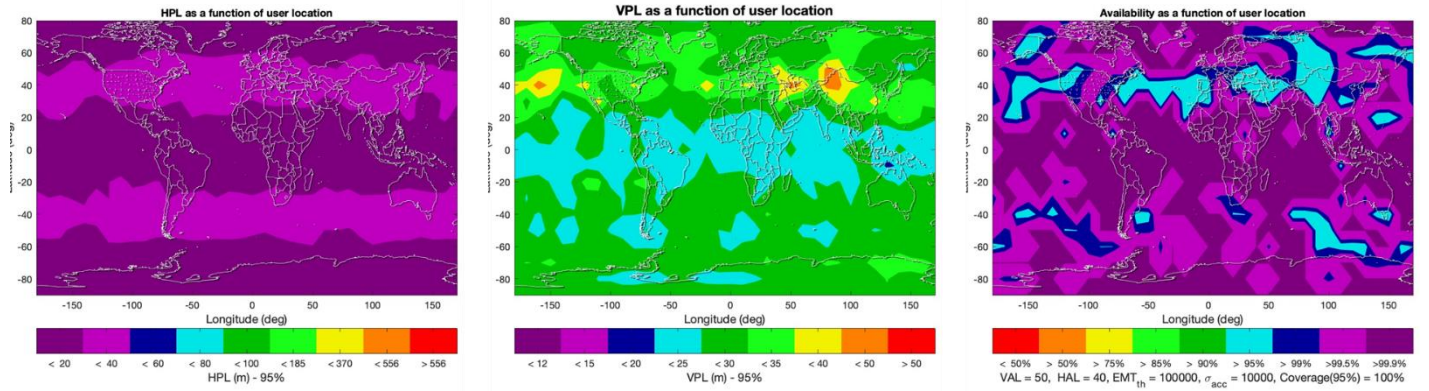
Figure 13: *HPL, VPL, and LPV Availability Contours for 24-Slot GPS Constellation and Alternative I-GEO Combination 1 ("3 × 3")*
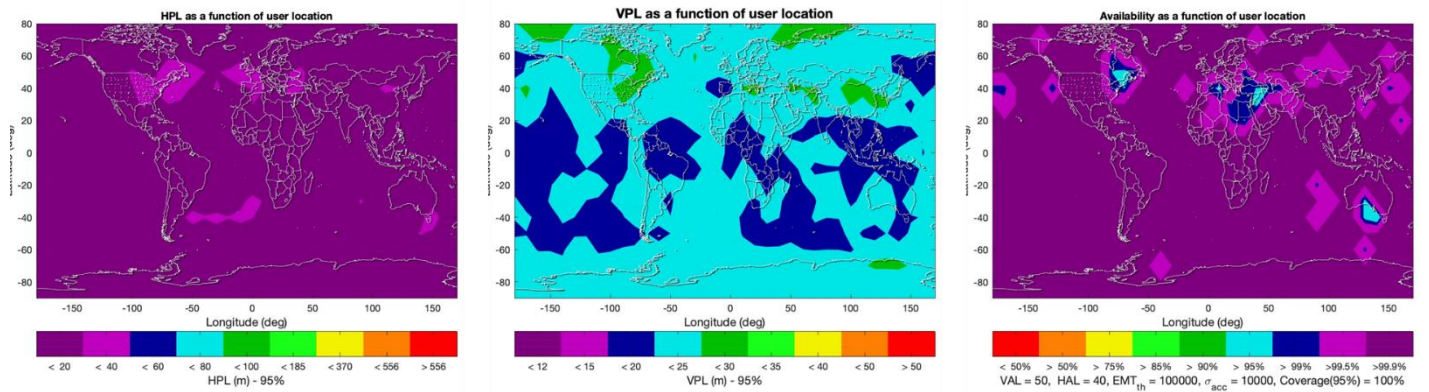

Figure 14: *HPL, VPL, and LPV Availability Contours for 30-Slot (24+6) GPS Constellation and Alternative I-GEO Combination 1 ("3 × 3")*
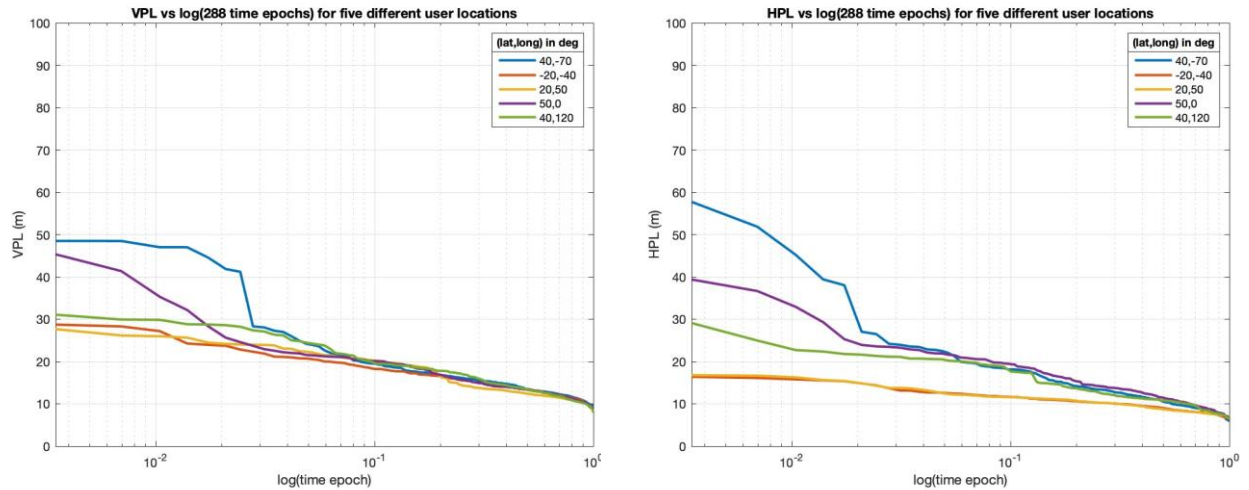

Figure 15: *Sorted VPL and HPL for 30-Slot (24+6) GPS Constellation and Alternative I-GEO Combination 1 ("3 × 3")*

4.4 GPS with Alternative I-GEO Combination 2 ("4 × 2")

The contour plots in Figures 16 and 17 are analogous to those in Figures 7 and 8 but for the eight-satellite, four-plane Alternative I-GEO Combination 2 as opposed to the baseline combination. These results are significantly better than those for Combination 1 due to the additional two I-GEO satellites. They are not quite as good as those of Alternative Combination 1, as this combination has one fewer satellite. Overall, the number of locations with LPV availability above 95% but below 99% is much larger for Alternative Combination 2 vs. 1 with the 24-Slot GPS constellation (Figure 15), and the same is true for locations with LPV availability above 99% but below 99.9% with the 30-Slot GPS constellation (Figure 16).

Figure 18 summarizes the sorted and unsorted results generated for this combination with a plot analogous to Figures 10 and 15 showing sorted VPL and HPL for the five selected locations shown in Table 4 and 30 GPS satellites. Overall, it is not very different from Figure 15 for Alternative Combination 1 but has slightly higher PLs, as suggested by the contour plots of Figures 16 and 17. Interestingly, the purple location at (50° N, 0° E) near London, UK is slightly better here than for Alternative Combination 1 but is still not as good as the baseline combination (with two fewer satellites). Overall, Figure 18 shows that VPL for these five locations is always below 60 meters and HPL is always below 50 meters (not considering satellite outages). However, three of these five locations have VPLs exceeding 35 meters (the LPV-200 VAL) for well over 1% of the simulated epochs, whereas this is only true of one location in Figure 15, Given these results, Alternative Combination 1 appears preferable to Alternative Combination 2, and the margin may be enough to justify the one additional satellite.
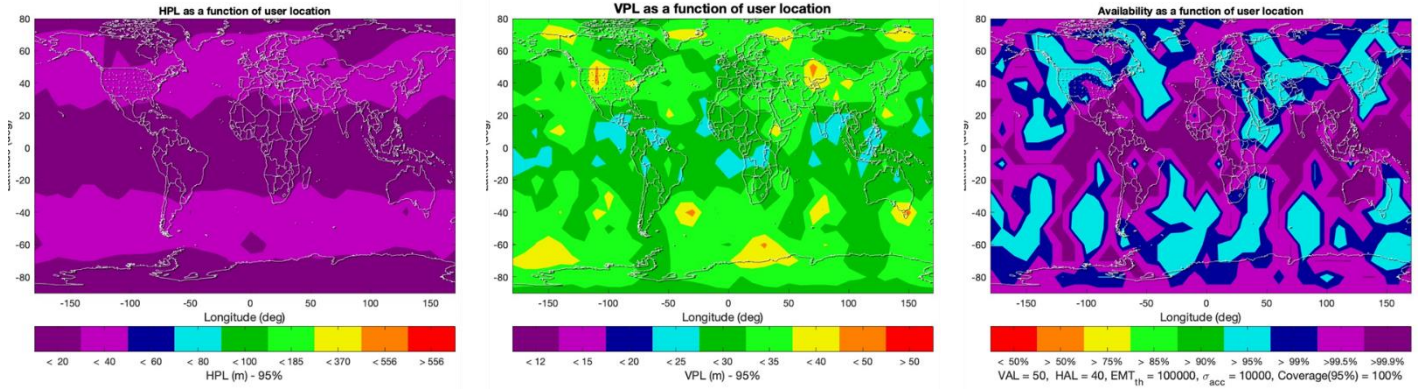

Figure 16: *HPL, VPL, and LPV Availability Contours for 24-Slot GPS Constellation and Alternative I-GEO Combination 2 ("4 × 2")*
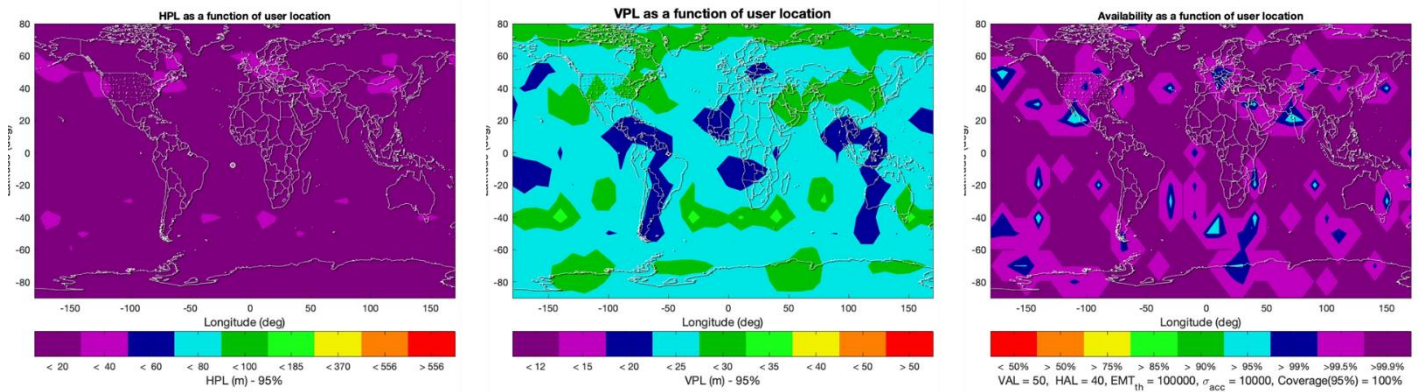

Figure 17: *HPL, VPL, and LPV Availability Contours for 30-Slot (24+6) GPS Constellation and Alternative I-GEO Combination 2 ("4 × 2")*
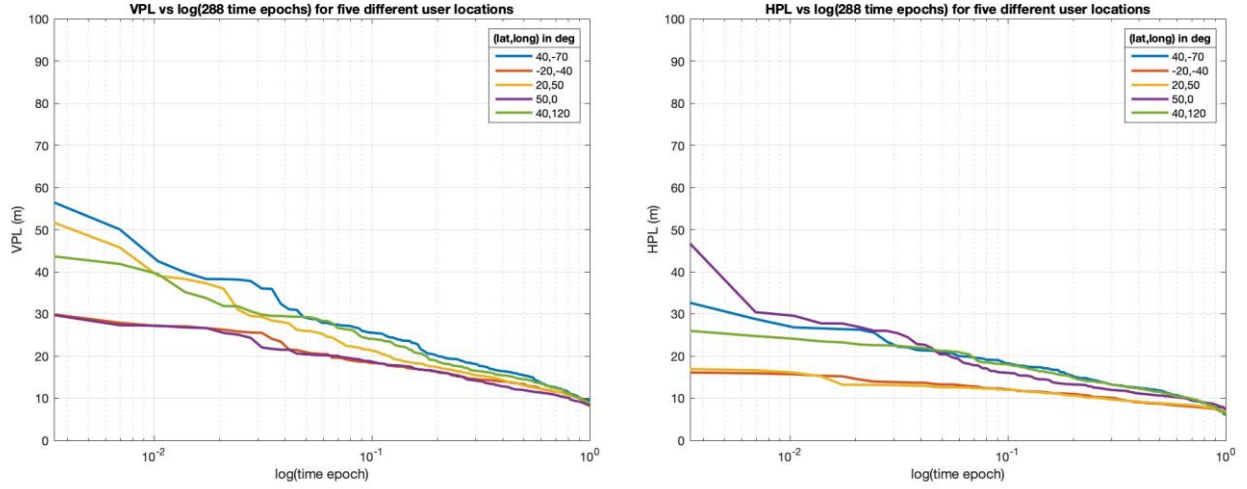
Figure 18: *Sorted VPL and HPL for 30-Slot (24+6) GPS Constellation and Alternative I-GEO Combination 2 ("4 × 2")*

5.   RESULTS FOR GPS AUGMENTENTED BY GLOBALSTAR LEO CONSTELLATION

MAAST ARAIM simulations have also been carried out with the 24 and 30-satellite GPS constellation variations augmented by existing LEO satellite constellations. Results are provided here for the Globalstar LEO constellation of telecommunications satellites, which can also be exploited to provide ranging measurements (see (Rabinowitz, 2000), (Pullen, 2018)). However, in order to provide ranging measurements with errors and fault probabilities similar to GPS, LEO constellations would most likely need to provide navigation signals as part of their mission design, as intended by the constellation being deployed by Xona Space Systems (Reid, 2021). The Globalstar LEO constellation is used here as a starting point because its relatively limited number of satellites reduces the total time needed for MAAST to simulate satellite positions and perform ARAIM calculations for the entire user grid. Globalstar is a good LEO constellation example because its signals are readily available (e.g., they can be utilized by iPhone 14 smartphones), it has been operated for over two decades, and it has recently been used for navigation as a signal of opportunity (Ardito, 2019).

The Globalstar satellite almanac used for this study was derived from the Celestrak online database (Celestrak) in early November 2022. It contains 85 satellites with a semi-major axis of roughly 8000 km (representing an altitude of about 1629 km above Earth's
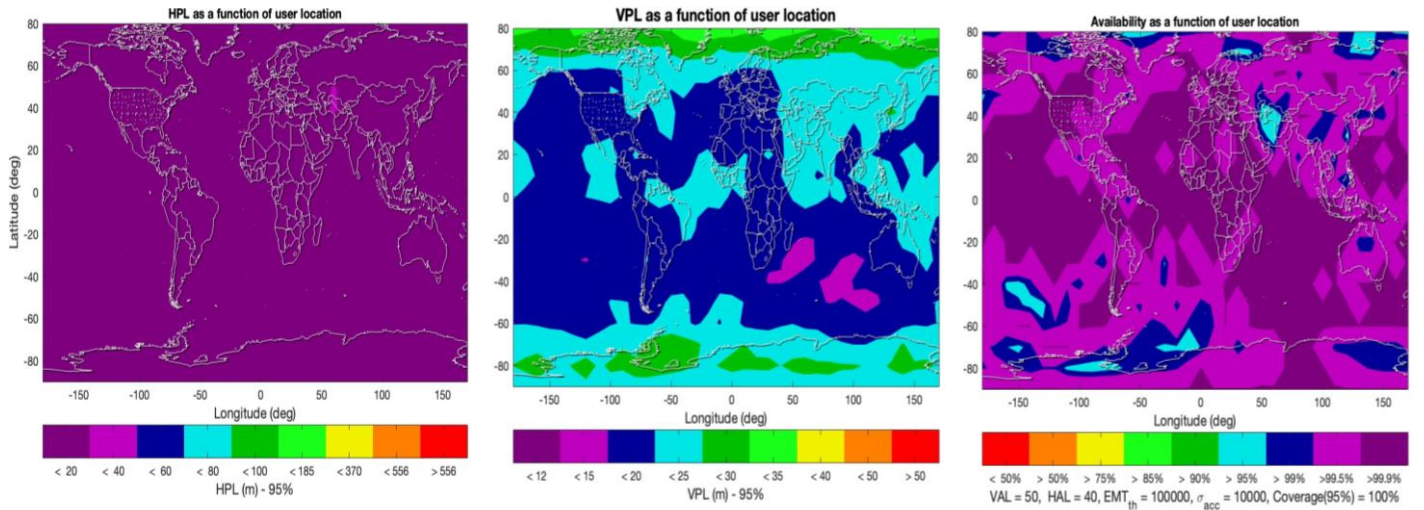

Figure 19: *HPL, VPL, and LPV Availability Contours for 30-Slot (24+6) GPS Constellation and Globalstar LEO Constellation*

mean radius of 6371 km), varying eccentricities (most below 0.2, but not quite circular orbits), and inclination angles of about 52 degrees (and thus similar to GPS and the I-GEOs). Not all these satellites are healthy in the Celestrak almanac, but they are all treated as healthy in MAAST ARAIM simulations. In addition, the navigation signals transmitted by Globalstar satellites are treated by MAAST as having the same range-error and fault-probability characteristics as GPS satellites in Figure 2, which is unrealistic at present. Therefore, the results of these simulations only show the potential for satellites in the simulated LEO orbits to augment GPS.

Figure 19 shows the 95% HPL, VPL, and LPV availability contours for the 30-slot (24+6) GPS constellation augmented by the 85-satellite Globalstar LEO constellation. As expected, the addition of GPS-quality LEO satellites improves the results greatly over the unaugmented 30-slot constellation shown in Figure 6. This improvement is broadly similar to (but not quite as good as) that obtained by Alternative I-GEO Combinations 1 and 2 in Figures 14 and 17, but the details are different. All user locations have LPV availability exceeding 95% and most exceeding 99.5%, but the number of locations with availability exceeding 99.9% (all epochs available) is significantly smaller than for Alternative I-GEO Combination 1. The difference appears to be due to slightly higher VPLs, especially near the poles, where the higher-altitude I-GEO satellites are visible to much larger areas.

Many different LEO satellite constellation configurations exist or are planned to be deployed over the next decade. The result for the recent (November 2022) Globalstar constellation in Figure 19 highlights the potential of LEO ranging satellite augmentation of GPS as an alternative or supplement to I-GEO augmentation, even without exploring the differential-carrier-phase integer ambiguity resolution advantages of LEO ranging satellites demonstrated in Rabinowitz (2000). ARAIM studies of additional LEO constellations are planned to further explore these possibilities.

6. SUMMARY, CONCLUSIONS, AND NEXT STEPS

This paper illustrates the potential for augmenting the GPS constellation with additional ranging satellites at inclined Geosynchronous orbits (I-GEO) and/or Low Earth Orbits (LEO). Our previous work in Pullen (2022) showed that a slight variation of the three-plane, six-satellite I-GEO constellation defined here as the baseline I-GEO combination provided excellent protection levels and LPV availability for dual-frequency SBAS users. Here, the focus is on ARAIM users who cannot exploit the SBAS corrections broadcast by the I-GEOs and thus depend upon the additional geometry redundancy provided by additional ranging satellites.

While GPS augmented by the six-satellite, three-plane baseline I-GEO combination provides very good vertical ARAIM results that are much improved over those from using GPS only, significantly better results are obtained from Alternative I-GEO Combinations 1 and 2 which have nine satellites in three planes and eight satellites in four planes, respectively. Between these, Alternative Combination 1 has slightly better performance and consistency (uniformity) over worldwide user locations. More study is needed to determine whether the advantages of these combinations are sufficient to justify an additional two or three satellites and whether the easier maintenance of the three-plane arrangement of Alternative Combination 1 justifies an additional satellite compared to the four-plane configuration of Alternative Combination 2. In addition, since the I-GEO combinations examined thus far are relatively minor variations of the original concept of Figure 3, I-GEO variations with orbit parameters that alter the figure-eight symmetry of those simulated here are worth studying.

The ARAIM results of augmenting GPS with a recent 85-satellite Globalstar LEO satellite constellation are also encouraging and are not very different from what is obtained from Alternative I-GEO Combinations 1 and 2. However, these results are based on LEO ranging signals equivalent to GPS (and I-GEO) in terms of signal-in-space errors and integrity fault probabilities. Simulations with additional LEO constellations, including those designed to transmit navigation signals with bounded range-domain errors, are needed to better understand the potential of LEO satellite augmentation. Combinations of I-GEO and LEO satellites (not including GPS or other GNSS satellites at Medium Earth Orbit or MEO) may also be of interest.

7. REFERENCES

(Ardito, 2019)   Ardito, C., Morales, J., et al., "Performance Evaluation of Navigation Using LEO Satellite Signals with Periodically Transmitted Satellite Positions," *Proceedings of ION ITM 2019,* Reston, VA, Jan. 2019, 306-318. https://doi.org/10.33012/2019.16743

(Blanch, 2015)   Blanch, J. et al. (2015), "Baseline advanced RAIM user algorithm and possible improvements," *IEEE Transactions on Aerospace and Electronic Systems*, 51(1), 713-732. https://10.1109/TAES.2014.130739

(Celestrak)   Celestrak Orbit Elements (website), https://celestrak.org/NORAD/elements/gp.php?GROUP=globalstar&FORMAT=tle

(ICAO, 2020)   "Proposed amendments to Annex 10, Volume I: Global Positioning System (GPS) provisions," ICAO Navigation Systems Panel (NSP), Sixth Meeting, WP 2, November 2020. https://store.icao.int/en/annexes/annex-10

(Katz, 2021)   Katz, A., Pullen, S., et al. (2021), "ARAIM for Military Users: ISM Parameters, Constellation-Check Procedure and Performance Estimates," *Proceedings of ION ITM 2021* (Virtual), 173-188. http://web.stanford.edu/group/scpnt/gpslab/pubs/papers/Katz_ION_ITM2021_Military_ARAIM.pdf

(MAAST)   "Matlab Algorithm Availability Simulation Tool," Stanford University GPS Laboratory, https://gps.stanford.edu/resources/tools/maast

(Milestone 3, 2016) "Milestone 3 Report of the E.U.-U.S. Cooperation on Satellite Navigation Working Group C: ARAIM Technical Subgroup," Final Version, Feb. 25, 2016. https://www.gps.gov/policy/cooperation/europe/2016/working-group-c/

(Pullen, 2018)   Pullen, S., Kilfeather, J., et al., "Enhanced Navigation, Robustness, and Safety Assurance for Autonomous Vehicles as Part of the Globalstar Connected Car Program," *Proceedings of ION GNSS+ 2018*, Miami, FL, Sept. 2018, 1538-1565. https://doi.org/10.33012/2018.16106

(Pullen, 2021)   Pullen, S., Lo, S., et al., "Ground Monitoring to Support ARAIM for Military Users: Alternatives for Rapid and Rare Update Rates," *Proceedings of ION GNSS+ 2021*, St. Louis, MO (Virtual), Sept. 2021 (presentation only). http://web.stanford.edu/group/scpnt/gpslab/pubs/papers/Pullen_IONGNSS_2021_Mil_ARAIM.pdf

(Pullen, 2022)   Pullen, S., Lo, S., et al., "Inclined Geosynchronous Satellite Augmentation to Maximize Availability of Integrity for Future SBAS and ARAIM Users," *Proceedings of ION ITM 2022*, Long Beach, CA, Jan. 2022 (presentation only). http://web.stanford.edu/group/scpnt/gpslab/pubs/papers/Pullen_ION_ITM_2022_Inclined_GEO_Integrity_Availability.pdf

(Rabinowitz, 2000) Rabinowitz, M., *A Differential Carrier-Phase Navigation System Combining GPS with Low Earth Orbit Satellites for Rapid Resolution of Integer Cycle Ambiguities*, Ph.D. Dissertation, Stanford University, Dept. of Aeronautics and Astronautics, December 2000. http://web.stanford.edu/group/scpnt/gpslab/pubs/theses/MatthewRabinowitzThesis01.pdf

(Reid, 2021)   Reid, T., "Opportunities in Commercial LEO Satellite Navigation," *Proceedings of ION GNSS+ 2021*, St. Louis, MO, Sept. 2021, 2012-2048. https://doi.org/10.33012/2021.18106

(SPS, 2020)   *GPS Standard Positioning Service (SPS) Performance Standard (GPS SPS PS)*, Washington DC, U.S. Dept. of Defense, 5th Edition, April 2020. https://www.gps.gov/technical/ps/2020-SPS-performance-standard.pdf